JOURNAL OF Applied Polymer SCIENCE

Polyamide 12 (PA12)/Clay Nanocomposites Fabricated by Conventional Extrusion and Water-Assisted Extrusion Processes

Karen Stoeffler, Leszek A. Utracki, Yves Simard, Sylvain Labonté
National Research Council of Canada, Boucherville, Quebec, Canada, J4B 6Y4
Correspondence to: K. Stoeffler (E-mail: karen.stoeffler@cnrc-nrc.gc.ca).

ABSTRACT: This work aims at comparing the efficiency of three melt compounding methods for preparing polyamide 12 (PA12)/untreated clay composites. Conventional extrusion was compared with two water-assisted extrusion methods previously described in the literature and respectively involving injection of water in the polymer/clay stream or injection of aqueous clay slurry in the polymer stream. The dispersion of the clay in the composites was analyzed at the microscale and at the nanoscale using microscopy (optical and electronic) and wide angle X-ray diffraction (WAXD). The tensile properties of the composites were evaluated. The results showed that injection of aqueous clay slurry in the polymer stream was the most efficient method for preparing PA12/untreated clay composites, although clay particles remained mainly dispersed at the microscale. This method allowed for a drastic size reduction of the microparticles, accompanied by enhancements of ca. +10 % in tensile modulus and tensile strength (compared with equivalent composites obtained by conventional extrusion). The influence of the pH of the aqueous clay slurry was also investigated: neutralization of the clay slurry generated finer dispersions, probably resulting from a better pre-exfoliation of the clay in the water medium. PA12/organophilic clay composites were also prepared as control samples. When an adequate surface treatment was selected, nanoscale dispersion of the clay platelets was easily achieved. In this case, composites prepared by conventional extrusion showed overall similar properties as their equivalents prepared using injection of water in the polymer/clay stream. © 2013 Wiley Periodicals, Inc. J. Appl. Polym. Sci. 130: 1959–1974, 2013

KEYWORDS: composites; clay; extrusion

Received 14 February 2013; accepted 9 April 2013; Published online 10 May 2013
DOI: 10.1002/app.39390

INTRODUCTION

Polymer nanocomposites based on natural clays have been the subject of numerous studies. Melt compounding, and more specifically twin-screw extrusion compounding, is currently the preferred preparation method since it allows for large scale production of thermoplastic-based nanocomposites. Exfoliation of the clay platelets at the nanoscale within the polymer matrix allows for significant mechanical reinforcement at relatively low clay loadings (1 wt % to 6 wt %). Nanoscale dispersions can be achieved using clays modified with a proper surface treatment. Cationic surfactants, and most commonly quaternary ammonium organic surfactants, are generally employed. Those surface treatments do not only improve the compatibility between the hydrophilic clay and the polymer matrix, but also increase the interlayer spacing of the clay, thereby weakening the attraction forces between individual platelets and facilitating their subsequent exfoliation. Despite their usefulness, the use of cationic modifiers presents certain drawbacks, including: (i) increased material cost, as surface modification contributes from 10 to 50% of total organoclay cost[1]; (ii) limited thermal resistance of the organic intercalating agent, possibly leading to its thermal degradation upon processing, thereby reducing clay dispersibility[2] and generating degradation by-products[3]; and (iii) possible migration of the intercalating agent out of the nanocomposite during service life, which can be a safety concern for specific applications such as food packaging.

In the last decade, significant effort has been devoted to the fabrication of polymer/untreated clay nanocomposites by melt processing techniques. Several authors have attempted to produce polymer/untreated clay nanocomposites by taking advantage of the natural affinities between water and untreated clay, using water as an *in situ* intercalating/exfoliating agent in the extrusion compounding process. The literature on water-assisted extrusion processes for the fabrication of polymer/clay nanocomposites is quite exhaustive. Two main methods have been developed. In 1999, Korbee and Van Geenen[4] described a process involving the injection of water (23 wt % of the total throughput in the extruder, Q_{tot}) in an extrusion stream

This article is dedicated to Leszek A. Utracki (1931–2012), a pioneer of National Research Council's Industrial Materials Institute (IMI).

Applied Polymer SCIENCE

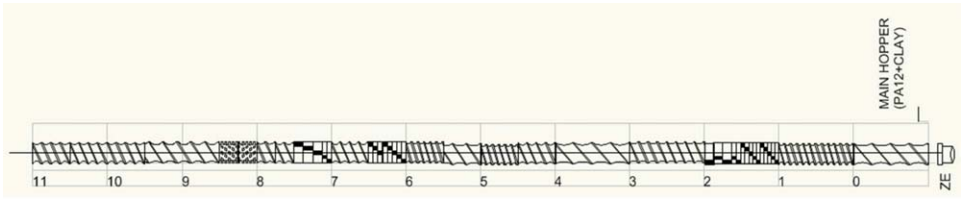

a) Method C (screw configuration 1)

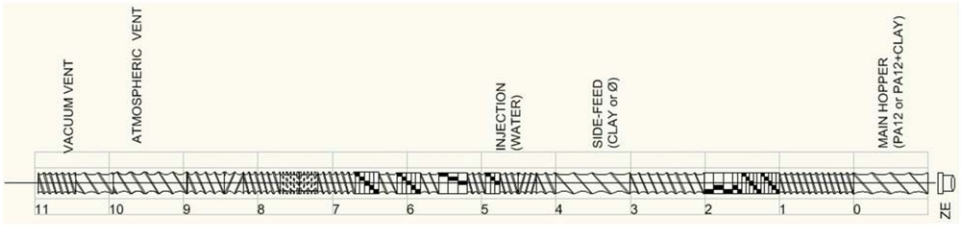

b) Method W (screw configuration 2)

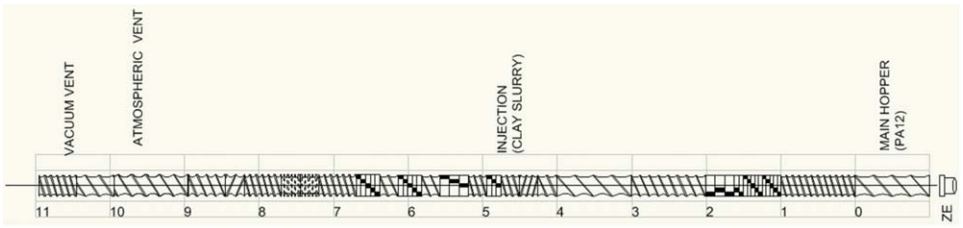

c) Method S (screw configuration 2)

Figure 1. Compounding strategies: (a) Method C (screw configuration 1); (b) Method W (screw configuration 2); (c) Method S (screw configuration 2). [Color figure can be viewed in the online issue, which is available at wileyonlinelibrary.com.]

composed of polyamide 6 (PA6) and untreated montmorillonite. They claimed that compared with conventional extrusion, their method significantly improved the dispersion of the clay platelets in PA6 and enabled a drastic enhancement of the heat deflection temperature. Their process was further applied by numerous authors to produce PA6,[5–8] polypropylene (PP) and

Table I. List of Prepared Formulations

#	Matrix	Clay	Clay feeding[a]	Organoclay (target) (wt %)	Inorganic content[b] (wt %)	Method—Screw configuration	Q_{tot} (kg/h)	Water (wt % Q_{tot})	$Q_{composite}$ (kg/h)
1	PA12	-	-	-	-	C—1	5	-	5
2	PA12	Cloisite Na^+	Dry powder—MH	5	4.54	C—1	5	-	5
3	PA12	Cloisite 30B	Dry powder—MH	6.65	4.75	C—1	5	-	5
5	PA12	-	-	-	-	C—2	5	-	5
6	PA12	-	-	-	-	W—2	6.1	18	5
7	PA12	Cloisite Na^+	Dry powder—MH	5	4.78	W—2	6.1	18	5
8	PA12	Cloisite Na^+	Dry powder—SF	5	4.90	W—2	6.1	18	5
14	PA12	Cloisite 30B	Dry powder—MH	6.65	4.57	W—2	6.1	18	5
13	PA12	Cloisite 30B	Dry powder—SF	6.65	4.63	W—2	6.1	18	5
17	PA12	Cloisite Na^+	Slurry (pH = 10)	5	4.04	S—2	6.1	40	3.7
18	PA12	Cloisite Na^+	Slurry (pH = 7)	5	4.48	S—2	6.1	40	3.7

[a] MH: main hopper; SF: side-feeder.

[b] As determined by TGA.

[c] For this processing method, hot spots at 250°C were observed in zones 6, 8, and 9 due to viscous dissipation.

maleated polypropylene (PP-*g*-MA),[9–12] styrene-acrylonitrile (SAN),[13] and copolyetheramide[14] composites based on untreated montmorillonite or other inorganic nanoparticles (e.g., halloysite nanotubes). Delamination of untreated montmorillonite at the nanoscale was readily achieved in PA6.[5–8] Using high pressure differential scanning calorimetry (HP-DSC), Fedullo et al.[7] showed that PA6 and water form a miscible system of high polarity and low viscosity under extrusion conditions (10 MPa/240°C), therefore increasing the dispersibility of untreated montmorillonite. This phenomenon is not likely to occur in the case of less polar matrices, explaining the limited success of this method with such matrices. For example, Rousseaux et al.[11] injected water (18 wt % Q_{tot}) in an extrusion stream composed of PP-*g*-MA and untreated montmorillonite but did not observe any enhancement in dispersion compared with conventional compounding. They attributed this result to a re-aggregation of the clay upon water removal, due to the high difference of polarity between untreated montmorillonite and PP-*g*-MA. Kato et al.[9] injected water (17 wt % Q_{tot}) in an extrusion stream composed of PP, untreated montmorillonite, a polymeric coupling agent (PP-*g*-MA) and an organic surfactant (trimethyl octadecyl ammonium chloride). They used a non standard extruder equipped with a long barrel (length : diameter = 77 : 1) enabling for long residence time. They reported fine nanoscale dispersions. The final composites exhibited mechanical properties comparable to those of equivalent composites produced by conventional compounding of PP, PP-*g*-MA, and montmorillonite modified with trimethyl octadecyl ammonium intercalating agents. However, although the authors show the feasibility of performing the cationic exchange directly in the extruder, their method does not eliminate the need for an organic modifier. In addition, no mention is made of the residual chloride counter-ions which might affect the thermal stability of the composites. The method developed by Korbee and Van Geenen[4] was also applied to the production of polymer nanocomposites based on organophilic montmorillonite. Rousseaux et al.[11] showed that injection of water in a PP-*g*-MA stream enhanced the dispersion of methyl tallow bis-2-hydroxyethyl modified montmorillonite (Cloisite 30B) compared with conventional compounding. They attributed this result to the occurrence of an esterification reaction between the hydroxyl functions of the intercalating agent and the carboxyl functions of PP-*g*-MA. Again, while this result is interesting, it does not eliminate the need for an intercalating agent. In 2003, a second type of water-assisted extrusion process was developed by Hasegawa et al.[15] The authors reported the fabrication of exfoliated PA6/untreated montmorillonite (1.6 wt %) nanocomposites via the injection of an untreated montmorillonite (2 wt %) aqueous slurry in an extrusion stream of PA6. According to the authors, when fed into the extrusion stream, the aqueous clay slurry is sheared apart into fine droplets containing pre-exfoliated clay platelets, which remain in their exfoliated state after elimination of water. Even at the low loadings used, Hasegawa et al.[15] reported appreciable enhancements in tensile properties (tensile modulus and strength increased by +37% and +21%, respectively), flexural properties (flexural modulus and strength increased by +12% and +14%, respectively) and heat deflection temperature (+27°C) compared with pure PA6. While the properties were comparable to those of PA6/organophilic montmorillonite (montmorillonite modified with octadecyl ammonium intercalating agents), the authors did not compare their materials with equivalent PA6/untreated montmorillonite composites prepared by conventional compounding. Despite the promising results reported, their strategy was not further investigated: most authors considered that the high viscosity of the aqueous clay slurry might be a concern for injection, and that the huge amount of water required (50 wt % Q_{tot}) was a limiting factor.

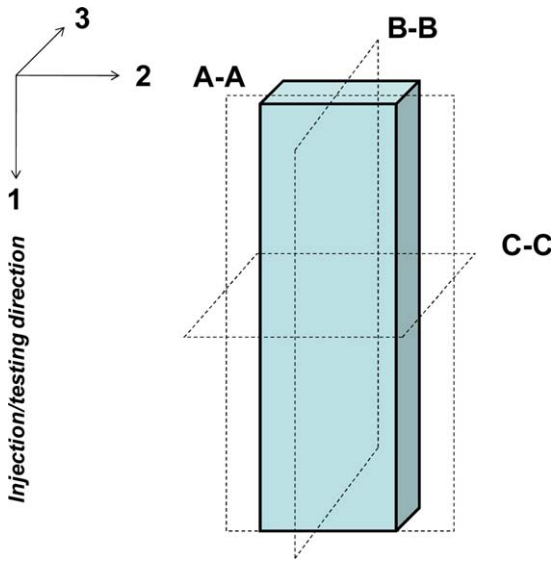

Figure 2. Schematics of the injection-molded specimens: tensile testing and injection directions are equivalent. Clay dispersion was analyzed by microscopy in the B-B plane. [Color figure can be viewed in the online issue, which is available at wileyonlinelibrary.com.]

The present work mainly aims at comparing the dispersion efficiency of conventional compounding and water-assisted processes. Polyamide 12 (PA12), which is widely used in food packaging and is approved by FDA for direct food contact application, was selected as the matrix. This polymer comprises both polar amide groups and long hydrophobic olefinic segments. PA12/untreated montmorillonite composites (5 wt %) were prepared using three compounding strategies: (i) conventional extrusion (referred to as Method C); (ii) injection of water in an extrusion stream composed of PA12 and montmorillonite (inspired by the method developed by Korbee and Van Geenen[4] and referred to as Method W); and (iii) injection of a montmorillonite aqueous slurry in a PA12 stream (inspired by the method proposed by Hasegawa et al.[15] and referred to as Method S). It should be noted that the method developed by Hasegawa et al.[15] was modified so as to produce final composites containing higher montmorillonite loadings while maintaining an acceptable water throughput in the extrusion stream (40 wt % Q_{tot}). Equivalent composites incorporating a commercial modified montmorillonite especially designed for compounding with polyamides were also prepared as control samples. The dispersion of the clay in the composites was analyzed at the microscale and at the nanoscale, and it was correlated to their tensile properties.

Applied Polymer SCIENCE

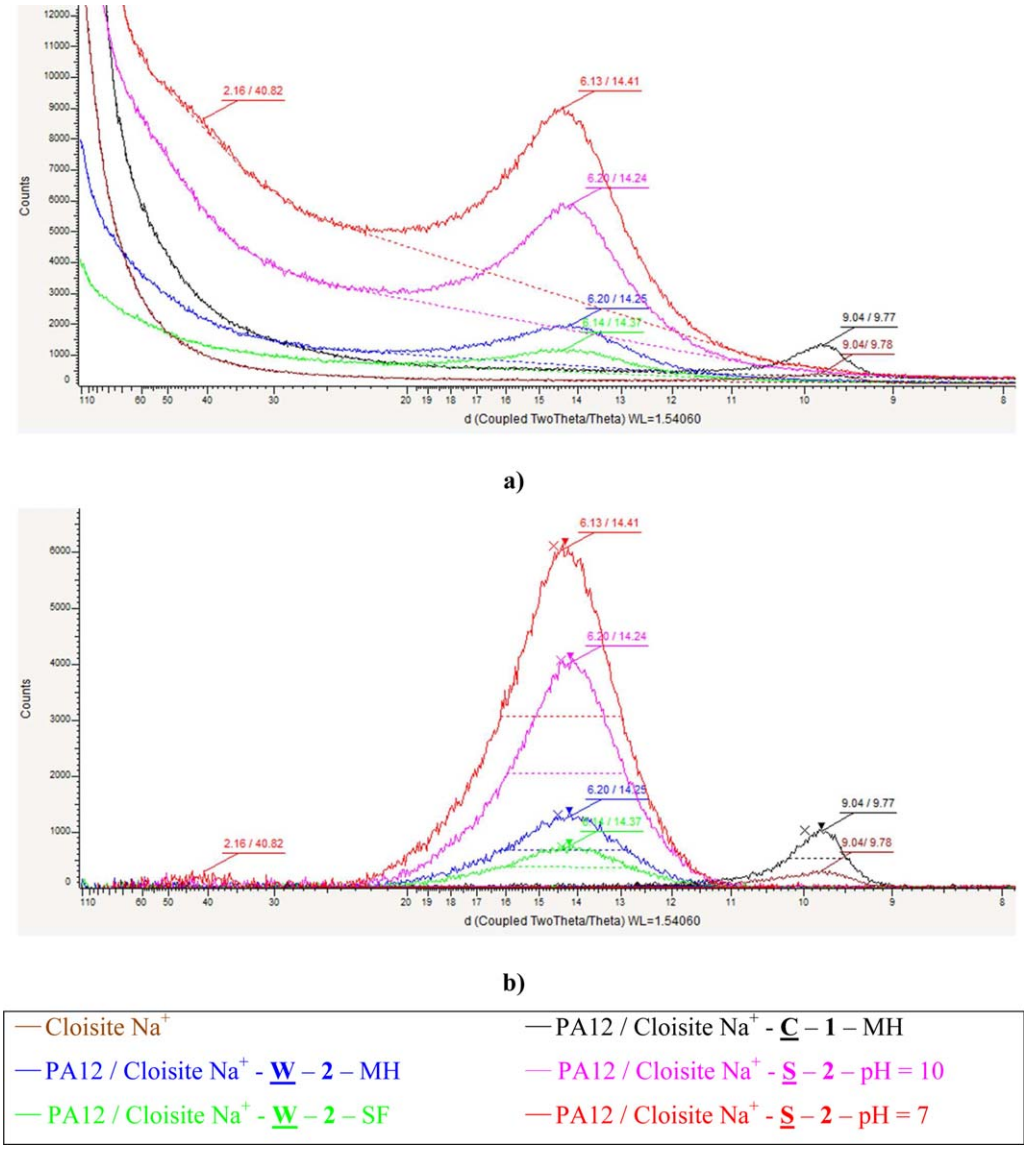

Figure 3. X-ray diffractograms of PA12/Cloisite Na^+ composites (horizontal axis corresponds to *d* in Å): (a) unsubtracted spectra; (b) background subtracted spectra. [Color figure can be viewed in the online issue, which is available at wileyonlinelibrary.com.]

Table II. Clay interlayer Spacing (d_{001}), Full Width at Half Maximum (FWHM), and Number of Platelets per Stack (N) as Calculated from XRD Diffractograms of PA12/Cloisite Na^+ Composites (Note: *N* is Valid only for Clay Particles Smaller Than 0.1 μm)

#	Sample	d_{001}(nm)	FWHM (degrees)	*N*
-	Cloisite Na^+	0.98	0.960	na
2	PA12/Cloisite Na^+—C—1—MH	0.98	0.659	13.4
7	PA12/Cloisite Na^+—W—2—MH	1.43	1.441	4.9
8	PA12/Cloisite Na^+—W—2—SF	1.44	1.412	4.9
17	PA12/Cloisite Na^+—S—2 (pH = 10)	1.42	1.312	5.2
18	PA12/Cloisite Na^+—S—2 (pH = 7)	4.08, 1.44	nd, 1.340	nd, 5.1

na: not applicable.
nd: not determined.

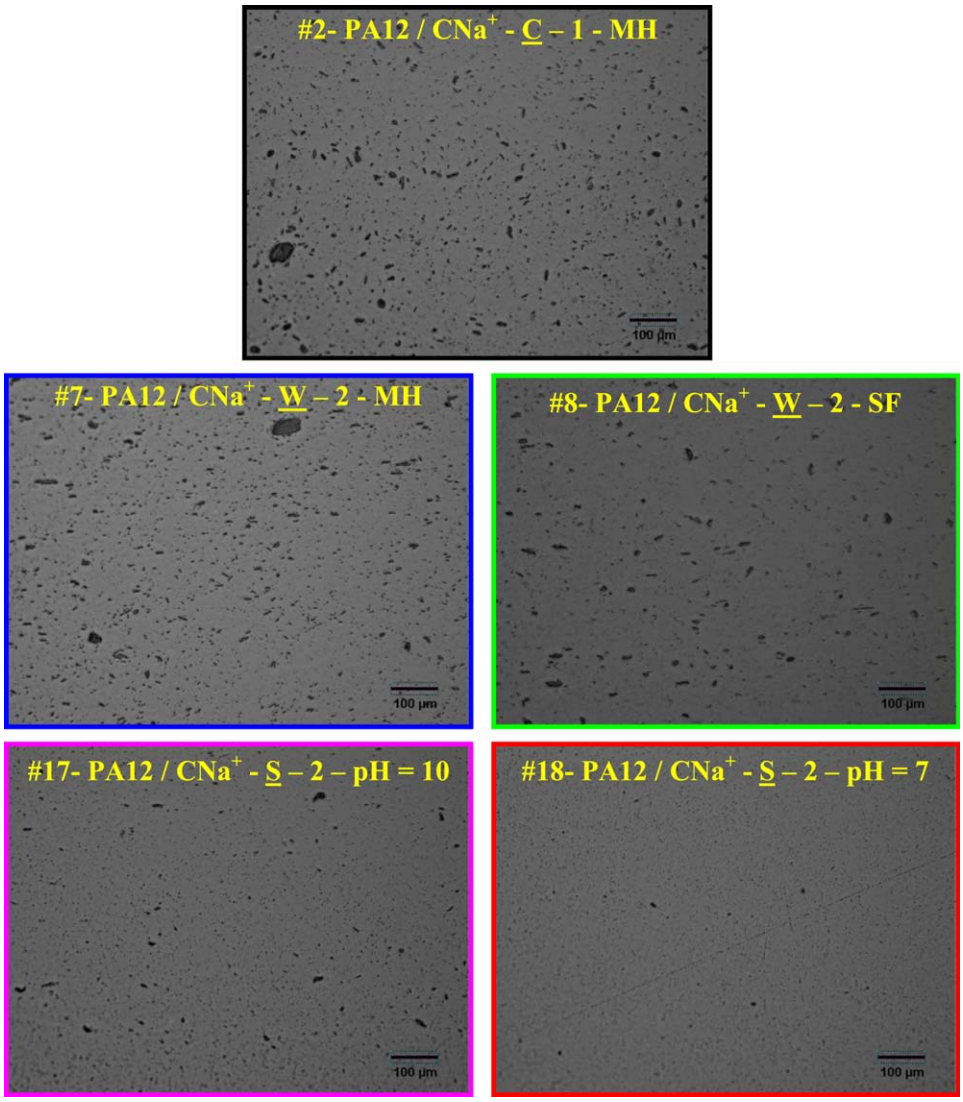

Figure 4. Optical micrographs of PA12/Cloisite Na^+ composites prepared using various compounding strategies. Method S clearly improves the dispersion at the microscale. [Color figure can be viewed in the online issue, which is available at wileyonlinelibrary.com.]

In addition to the major objective aiming at comparing the various processing methods, specific parameters were studied. First, the influence of clay feeding location (main hopper feeding versus side feeding) was investigated for Method W. Indeed, this parameter is susceptible to play a role in the dispersion process. Main hopper feeding allows for longer residence time in the extruder, then favoring diffusion of the polymer chains in the clay galleries. However, side feeding just before the water injection point might facilitate contact between undispersed clay and water, hence leading to a better intercalation of the clay galleries by water molecules. Second, the effect of the pH of the aqueous slurry was evaluated for Method S. Indeed, colloidal behavior of aqueous montmorillonite suspensions is known to be strongly affected by pH. While montmorillonite faces have permanent negative charges (resulting from isomorphic substitutions in the lattice), their edges have pH dependent charges. Adsorption of sufficient amounts of protons at the edges creates positive charges, promoting face-to-edge arrangements in the suspension and resulting in the formation of house of cards type networks.[16–18] Therefore, it is thought that a decrease of the pH of the aqueous slurry will promote the formation of an exfoliated tridimensional network of montmorillonite platelets, possibly leading to an improved dispersion of the montmorillonite in the resulting composite.

MATERIALS

A high viscosity PA12 commercial grade (melt volume rate: 20 cm^3/10 min at 275°C/5 kg; melting temperature: 178°C; density: 1.01 g/cm^3; M_w = 60,000 g/mol) was selected as the matrix. Cloisite Na^+, a natural montmorillonite with a cationic exchange capacity of 92.6 meq/100 g, and Cloisite 30B, a natural montmorillonite modified with a methyl tallow bis-2-hydroxyethyl quaternary ammonium salt (intercalating agent

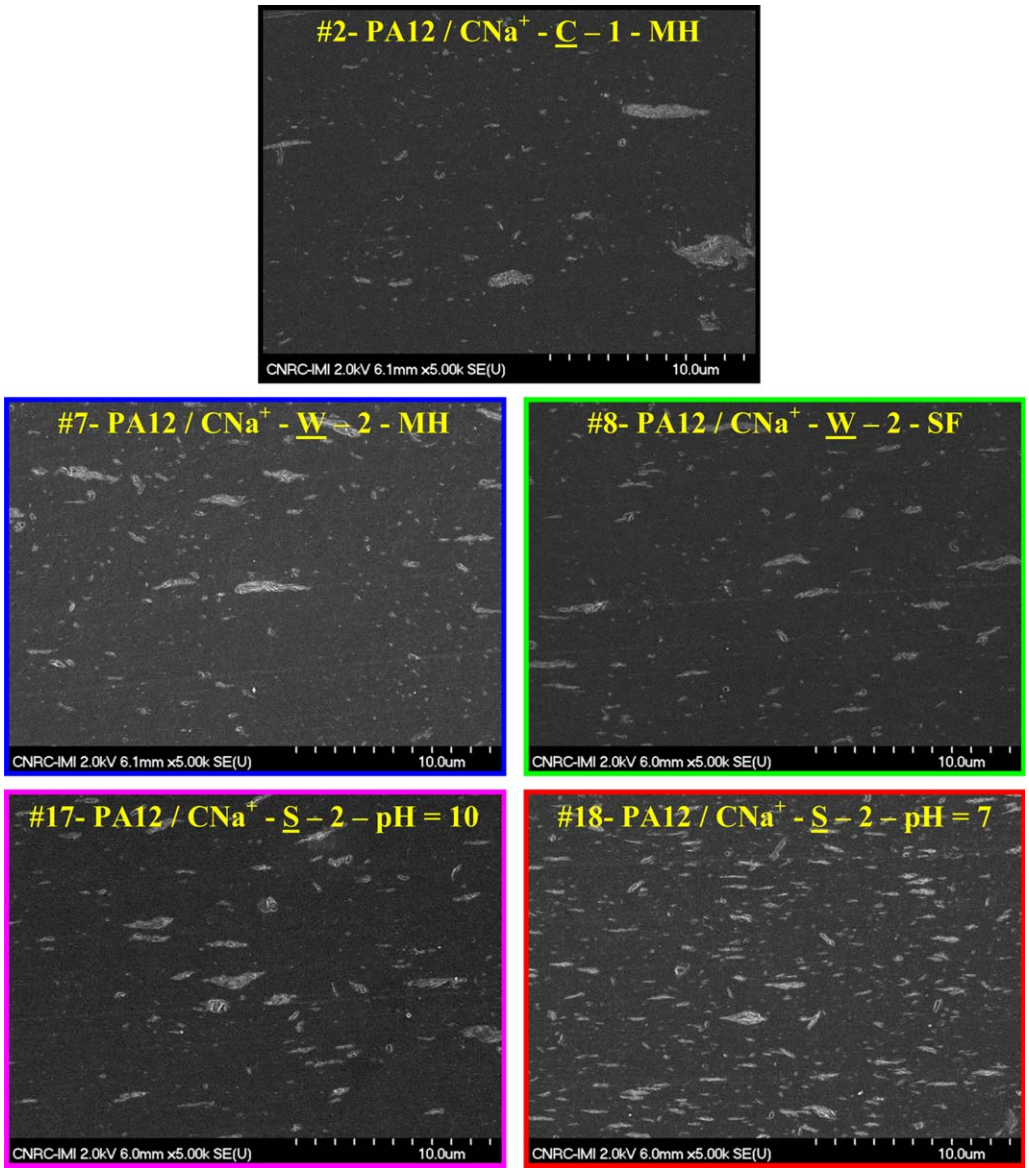

Figure 5. SEM photographs of PA12/Cloisite Na^+ composites prepared using various compounding strategies. Method S at neutral pH clearly improves the dispersion at the submicron scale. [Color figure can be viewed in the online issue, which is available at wileyonlinelibrary.com.]

concentration: 90 meq/100 g; recommended for compounding with polyamides), were purchased from Southern Clay Products. Hydrochloric acid (1 mol/L) was obtained from Fisher.

EXPERIMENTAL

Preparation of Aqueous Clay Slurries (Method S)

In view of producing PA12/untreated montmorillonite composites using Method S, aqueous Cloisite Na^+ (7 wt %) slurries were prepared. This concentration is significantly higher than that used by Hasegawa et al.[15] It was chosen so as to reach the target clay concentration (5 wt %) in the final composites while maintaining an acceptable water throughput (40 wt % Q_{tot}). In return, this concentration leads to a higher viscosity of the slurry and probably to a lower extent of pre-exfoliation of the clay platelets. In a typical procedure, Cloisite Na^+ (140 g; previously dried overnight at 80°C under vacuum) was slowly incorporated in deionized water (1860 mL) using a T50 Ultra Turrax® (Ika) high performance disperser operated at 4000 rpm. After complete incorporation of the clay, mixing was performed for 20 min. Homogeneous aqueous slurry (2 kg) was produced. A Fisher Scientific pH-meter, calibrated with three buffer solutions of pH 10.0, 7.0, and 4.0, was used to measure the natural pH of the slurry: a value of ca. 10 at 25°C was recorded. The process was repeated to prepare an additional batch (2 kg) of aqueous clay slurry of similar concentration. In this case, hydrochloric acid was slowly added after the mixing until a pH of ca. 7 was reached. Lower pH values were not investigated since a too high amount of protons might result in possible damage to the extrusion equipment. Aqueous clay slurries were allowed to rest at ambient temperature for 24 h, leading to partial gelation. One hour before extrusion, the tridimensional

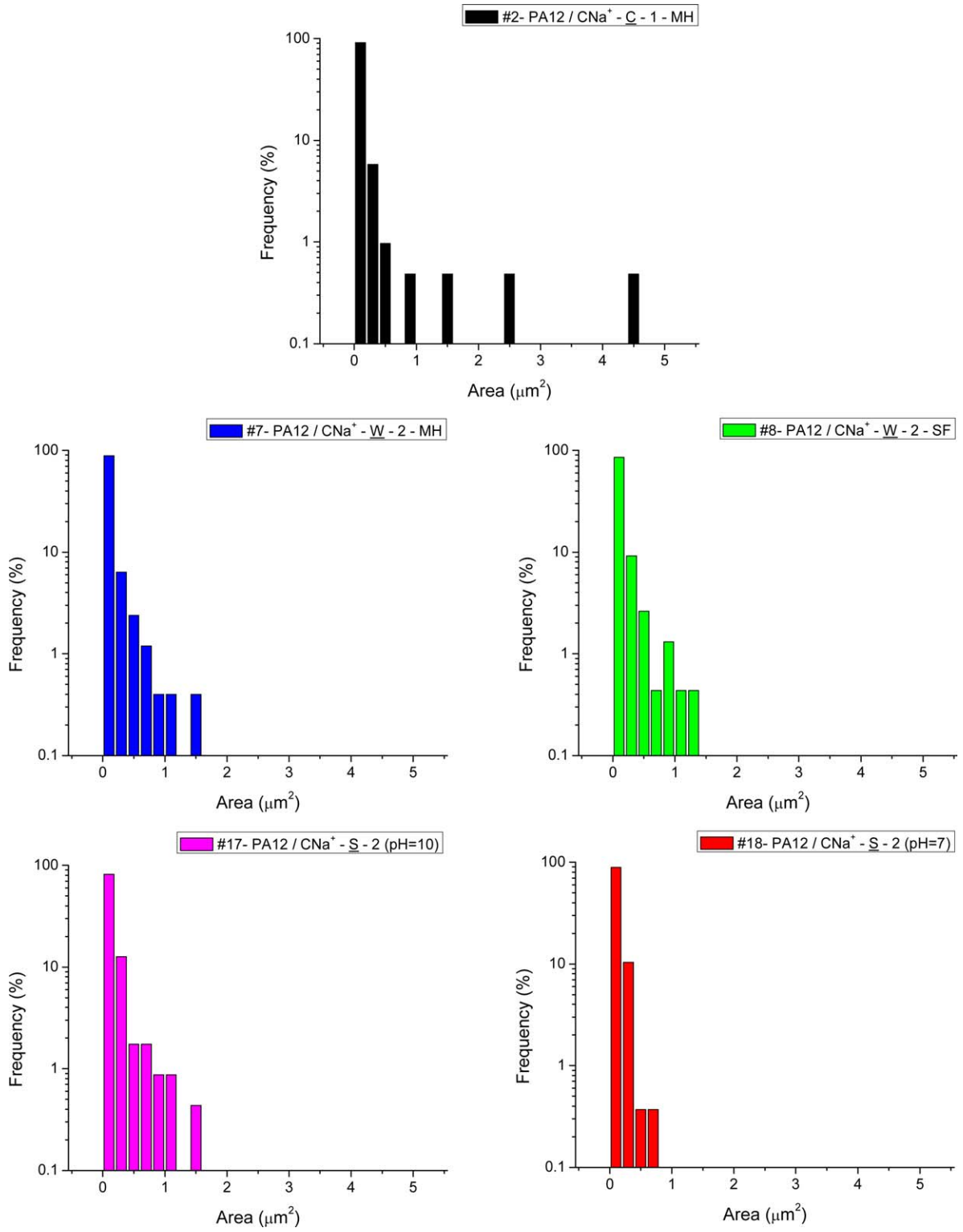

Figure 6. Area distribution of clay microparticles detected on SEM photographs (magnification of ×5000). Method S at neutral pH clearly reduces the size of the microaggregates. [Color figure can be viewed in the online issue, which is available at wileyonlinelibrary.com.]

clay structure in formation was disrupted using high shear mixing at 4000 rpm for 5 min, hence decreasing the viscosity and facilitating further pumping and injection in the extrusion stream.

Compounding of PA12/Clay Composites

PA12 and powdery clays were dried under vacuum at 80°C for 24 h before processing. Melt compounding was performed using

Table III. Descriptive Statistics of Clay Microparticles Population as Detected by Image Analysis on SEM Photographs of PA12/Cloisite Na^+ Composites (Magnification: 5000×)

	#2 C—1—MH	#7 W—2—MH	#8 W—2—SF	#17 S—2 (pH = 10)	#18 S—2 (pH = 7)
Particles counted	207	251	229	229	539
Density of particles (μm^{-2})	0.473	0.574	0.523	0.523	1.232
Mean area (μm^2)	0.076	0.060	0.068	0.082	0.041
Standard deviation (μm^2)	0.362	0.144	0.157	0.177	0.065
Lower 95% CI (μm^2)	0.026	0.042	0.048	0.059	0.035
Upper 95% CI (μm^2)	0.125	0.078	0.089	0.105	0.046
Minimum area (μm^2)[a]	0.005	0.005	0.005	0.005	0.005
Median area (μm^2)	0.016	0.019	0.016	0.018	0.016
Maximum area (μm^2)	4.362	1.325	1.273	1.404	0.680
Mean aspect ratio	1.951	1.877	2.022	2.093	2.138
Standard deviation	0.726	0.725	1.010	0.997	0.960
Lower 95% CI	1.852	1.787	1.890	1.964	2.056
Upper 95% CI	2.050	1.967	2.153	2.223	2.219
Minimum aspect ratio	1.153	1.196	1.075	1.156	1.119
Median aspect ratio	1.792	1.688	1.700	1.764	1.844
Maximum aspect ratio	5.612	6.182	8.493	6.875	10.5

[a] Minimum value was imposed as particles smaller than 0.005 μm^2 were excluded from statistical analysis.

a Leistritz 34 mm co-rotating twin-screw extruder comprising eleven zones. The three compounding strategies used (Method C, Method W, and Method S) are illustrated in Figure 1. For all compounding strategies, PA12 was fed at the main hopper. For Method C, powdery clay was fed at the main hopper. For Method W, powdery clay was fed either at the main hopper or downstream in zone 4 (side feeder). For Method S, aqueous clay slurry was injected in zone 5. Two screw configurations were used. Configuration 1 was applied to Method C. This medium shear configuration was developed based on the work of Dennis et al.,[19] who showed that efficient melt compounding of polymer/clay nanocomposites requires a combination of high shear (to break clay microaggregates apart into tactoids) and mild shear (to allow for polymer intercalation in the tactoids and for tactoids peeling). Thus, configuration 1 comprises: (i) a section of dispersive mixing elements to ensure polymer melting (zone 2); (ii) a section of dispersive and distributive mixing elements to ensure proper clay dispersion/distribution in the matrix (zones 7 to 9); (iii) conveying elements (zones 9 to 11) to allow for polymer diffusion. Configuration 2 was specifically built for Methods W and S. This configuration comprises: (i) a section of dispersive mixing elements (zone 2) identical as the one used in configuration 1; (ii) a sealing ring to avoid backflow of the injected liquid (end of zone 4); (iii) an injection port for water or aqueous clay slurry (zone 5); (iv) a section of intensive dispersive and distributive mixing (zones 6 to 8) especially designed to increase local pressure so as to maintain water in a liquid state[7,10–13]; (v) an atmospheric vent (zone 10) and a vacuum vent (zone 11) to remove residual water. For Method W, the water throughput was set at 18 wt % Q_{tot}, based on literature data.[4–7,9,11,13] For Method S, the water throughput was determined by the aqueous clay slurry concentration and the target clay concentration in the final composite. This resulted in a value of 40 wt % Q_{tot}. For all compounding strategies, the extruder was operated at a screw speed of 150 rpm and at temperatures comprised between 240°C and 245°C. The dry composite throughput ($Q_{composite}$) was maintained at 5 kg/h except in the case of Method S, for which torque limitations imposed a lower throughput (3.7 kg/h). The material was extruded through a double capillary die, air cooled and pelletized.

The composites pellets were dried under vacuum at 80°C for 24 h. Tensile test specimens were molded from those pellets using a Boy injection molding press (34 tons) operating between 215°C and 240°C. A thermogravimetric analyzer TGA/DSC1 (Mettler Toledo) was used to verify the actual inorganic content in injection-molded composites. Heating was applied from 25°C to 700°C at 20°C/min under nitrogen atmosphere. The residue was determined at 700°C. A complete list of the samples prepared is given in Table I.

Characterization of PA12/Clay Composites

Clay Dispersion. Clay dispersion in the composites was first analyzed by microscopy in the B-B plane, as shown in Figure 2. The presence of large aggregates was assessed on polished samples using a Leica optical microscope in reflection mode. At the microscale, clay dispersion was analyzed on cryomicrotomed samples using a FEG-SEM Hitachi S4700 electron microscope operating at 2 kV. Prior to observation, samples were coated with a vapour platinum deposit. Finally, at the nanoscale, clay dispersion was analyzed using transmission electron microscopy (TEM) and wide angle X-ray diffraction (WAXD). TEM observations were done on cryoultramicrotomed lamellae of thickness ca. 80 nm using a JEOL JEM 2100F microscope operating at 200 kV. X-ray

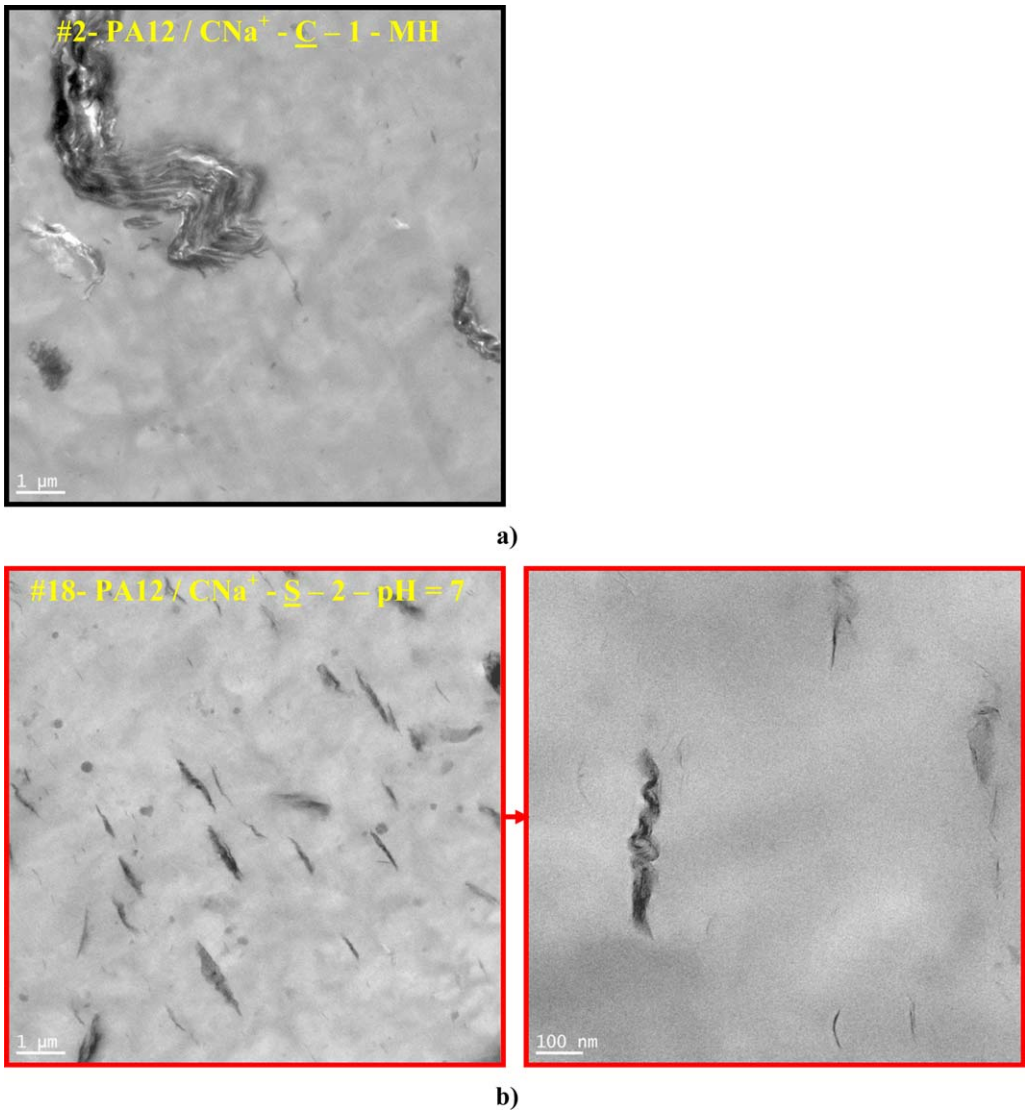

Figure 7. TEM photographs of PA12/Cloisite Na^+ composites prepared using: (a) Method C; (b) Method S (pH = 7). Method S at neutral pH produces a higher density of submicron and nanoparticles than Method C. [Color figure can be viewed in the online issue, which is available at wileyonlinelibrary.com.]

diffractograms were obtained with a Bruker D8 Discover high resolution X-ray diffractometer operating at 40 kV and 40 mA ($Cu_{K\alpha}$ radiation; λ = 0.1514 nm). The spectra were obtained in reflexion mode between 0.8° and 10°, using a step increment of 0.015° and an acquisition time of 1.5 s/point. For analysis, background subtraction was performed using the DIFFRAC^{plus} EVA software (Bruker). The interlayer spacing (d_{001}) and the full width at half maximum (FWHM) of the clay diffraction peak were determined.

Oscillatory Rheometry. The rheological properties of unprocessed PA12, extruded PA12, and selected PA12/clay composites were measured using an Ares strain controlled rheometer equipped with 25 mm parallel plates. Prior to testing, polymers and composites pellets were dried under vacuum at 80°C for 24 h to remove residual moisture. Frequency sweep measurements between 0.1 rad/s and 100 rad/s were carried out at 230°C in a nitrogen atmosphere under a constant strain of 15% (as determined from preliminary strain sweep measurements).

Tensile Properties. Tensile properties of the composites were measured on type I injection-molded specimens according to standard ASTM D638. Samples were conditioned at 50°C under vacuum for 40 h before testing. An Instron 1123 machine equipped with a 25 kN load cell was used. Specimens were drawn at a crosshead speed of 50 mm/min. The tensile modulus (E) was measured using an extensometer (50 mm, 10 %). Maximum tensile stress (σ_{max}) and elongation at break (ε_b) were also determined. Values reported are the average of 5 measurements per formulation.

RESULTS AND DISCUSSION

Clay Dispersion in PA12/Cloisite Na^+ Composites

WAXD diffractograms of PA12/Cloisite Na^+ composites are shown in Figure 3. All composites exhibit clear diffraction

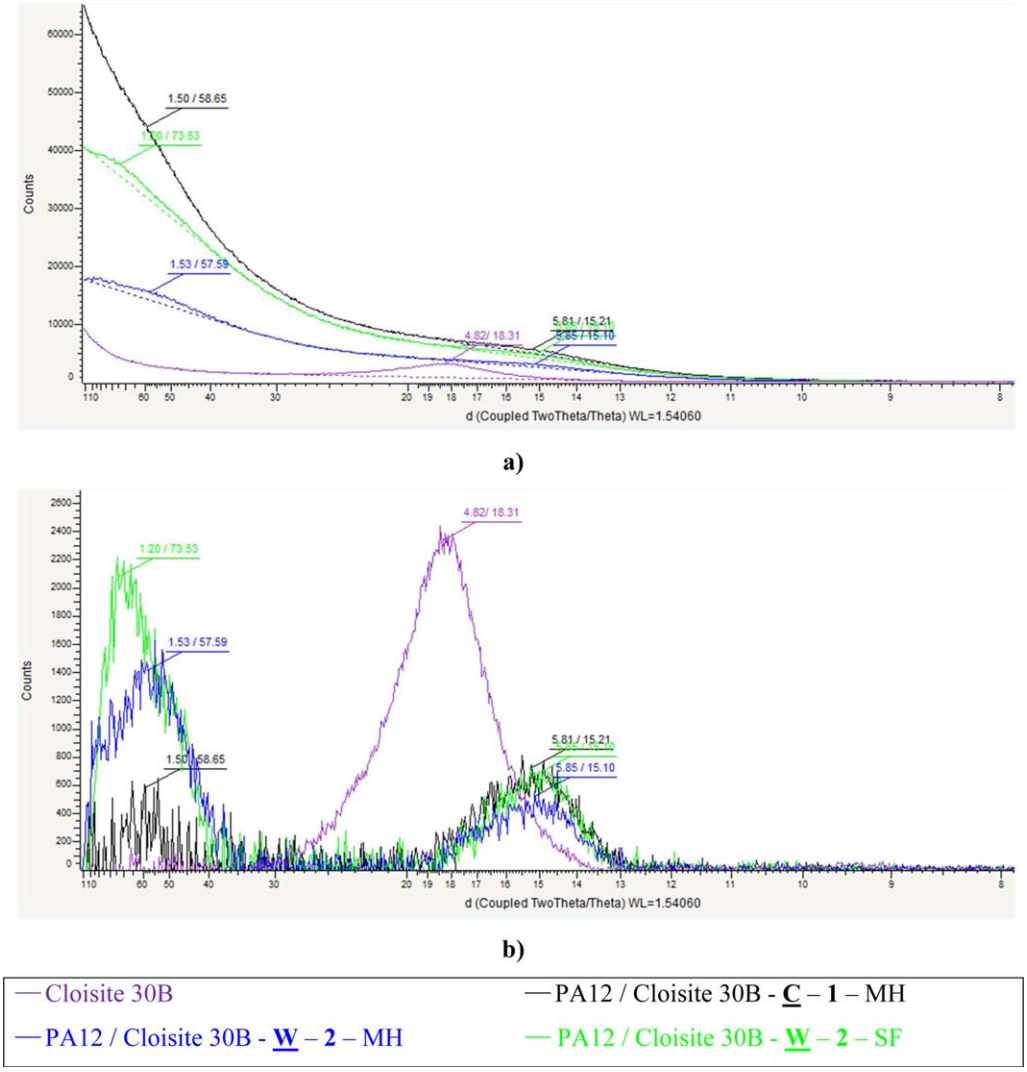

Figure 8. X-ray diffractograms of PA12/Cloisite 30B composites (horizontal axis corresponds to *d* in Å): (a) unsubtracted spectra; (b) background subtracted spectra. [Color figure can be viewed in the online issue, which is available at wileyonlinelibrary.com.]

peaks, typical of microcomposite or intercalated nanocomposite structures. Composites processed using Method C (d_{001} = 0.98 nm) do not show any modification of the clay interlayer spacing compared with pure Cloisite Na^+ (d_{001} = 0.98 nm), indicating that no intercalation took place. On the contrary, composites processed using Method W exhibit a significant expansion of the interlayer distance (d_{001} = 1.42 nm–1.43 nm; equivalent to the intercalation of one to two water layers[20]) with a broadening and an increase in intensity of the clay diffraction peak. Composites prepared with Method S show a similar clay interlayer distance (d_{001} = 1.42 nm–1.44 nm) accompanied by an additional increase in intensity of the diffraction peak. Additionally, composites fabricated from the neutralized clay slurry (pH = 7) show a small diffraction peak at 2.2° (equivalent to 4.1 nm), possibly indicating some extent of exfoliation. For all composites, the

Table IV. Clay Interlayer Spacing (d_{001}), Area of the Clay Diffraction Peak (A), and Degree of Exfoliation (X_E) of PA12/Cloisite 30B Composites

#	Sample	d_{001}(nm)	A (counts × degrees)	X_E (%)
-	Cloisite 30B	1.83	1470.0	-
3	PA12/Cloisite 30B—C—1—MH	5.87, 1.52	262.0	82
14	PA12/Cloisite 30B—W—2—MH	5.76, 1.51	264.0	77
13	PA12/Cloisite 30B—W—2—SF	7.35, 1.51	343.9	82

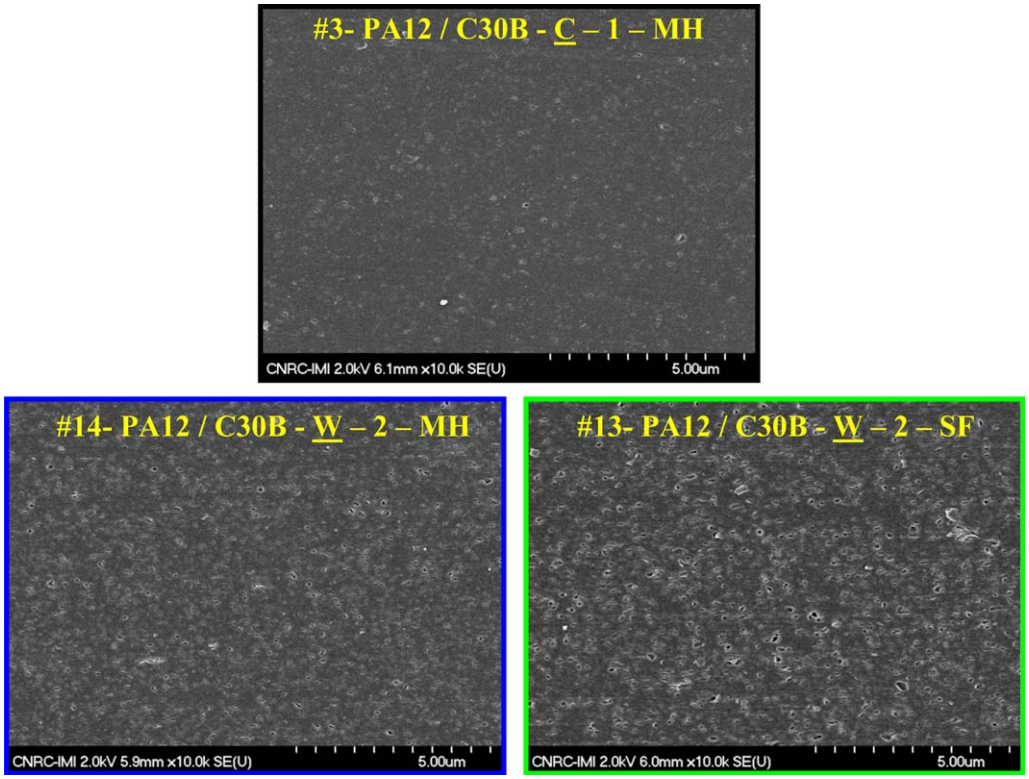

Figure 9. SEM photographs of PA12/Cloisite 30B composites prepared using various compounding strategies. Fine micro and submicron dispersions are observed for all samples. [Color figure can be viewed in the online issue, which is available at wileyonlinelibrary.com.]

Scherrer equation[21] was used to estimate the number of platelets (N) in tactoids:

$$N-1=\frac{K\,\lambda}{\mathrm{FWHM}.d_{001}.\cos\theta} \quad (1)$$

where $K \approx 0.9$, FWHM is the full width of the diffraction peak at half maximum (expressed in radians) and θ is the angle of beam incidence corresponding to the peak position. It should be noted that the Scherrer equation is not applicable to particles larger than 0.1 μm (hence, N corresponds to the number of platelets in tactoids smaller than 0.1 μm, and does not represent the number of platelets in larger aggregates). The results, shown in Table II, confirm that water-assisted extrusion processes lead to a drastic reduction of the number of platelets per stack in nanoscale tactoids: N decreases from ca. 13 in composites processed with Method C to ca. 5 for composites processed with Method W and Method S.

Optical micrographs of PA12/Cloisite Na^+ composites are shown in Figure 4. The macrodispersion is very similar for composites prepared with Method C and Method W. However, significant improvements are observed for composites prepared with Method S, which show a finer dispersion, especially when prepared from the neutralized clay slurry. SEM micrographs of PA12/Cloisite Na^+ composites are shown in Figure 5. Image analysis was performed using the Clemex Vision PE software to obtain quantitative information on clay microparticles. The frequency distribution of clay particles area (Figure 6) and the descriptive statistics for clay particles geometry (Table III) clearly show an increase in the density of the microparticles accompanied by a size reduction for composites fabricated using water-assisted extrusion processes. Method W (independently of the position of clay feeding) and Method S (pH = 10) give very similar dispersion states, with a density of 0.52 to 0.57 microparticles/μm^2 (compared with 0.47 microparticles/μm^2 for Method C) and microaggregates no larger than 1.3 μm^2 to 1.4 μm^2 (compared with 4.4 μm^2 for Method C). Further enhancement is obtained by combining Method S and neutralization of the clay slurry, leading to an increased density of 1.23 microparticles/μm^2, with microaggregates no larger than 0.7 μm^2. Overall, a 46% reduction of clay microparticles area is observed for composites prepared using Method S (pH = 7) compared with composites prepared using Method C. This size reduction is also obvious at the submicroscale, as observed on TEM photographs (Figure 7). In addition, very thin tactoids and single platelets can also be observed in this particular formulation, consistent with the small diffraction peak observed at 4.1 nm by WAXD. Despite the significant decrease in clay microparticles area obtained using water-assisted extrusion methods, the aspect ratio of clay microparticles remains fairly low for all PA12/Cloisite Na^+ composites, varying from 1.95 (Method C) to 2.14 [Method S (pH = 7)].

Clay Dispersion in PA12/Cloisite 30B Composites

WAXD diffractograms of PA12/Cloisite 30B composites are shown in Figure 8. Compared with pure Cloisite 30B, all

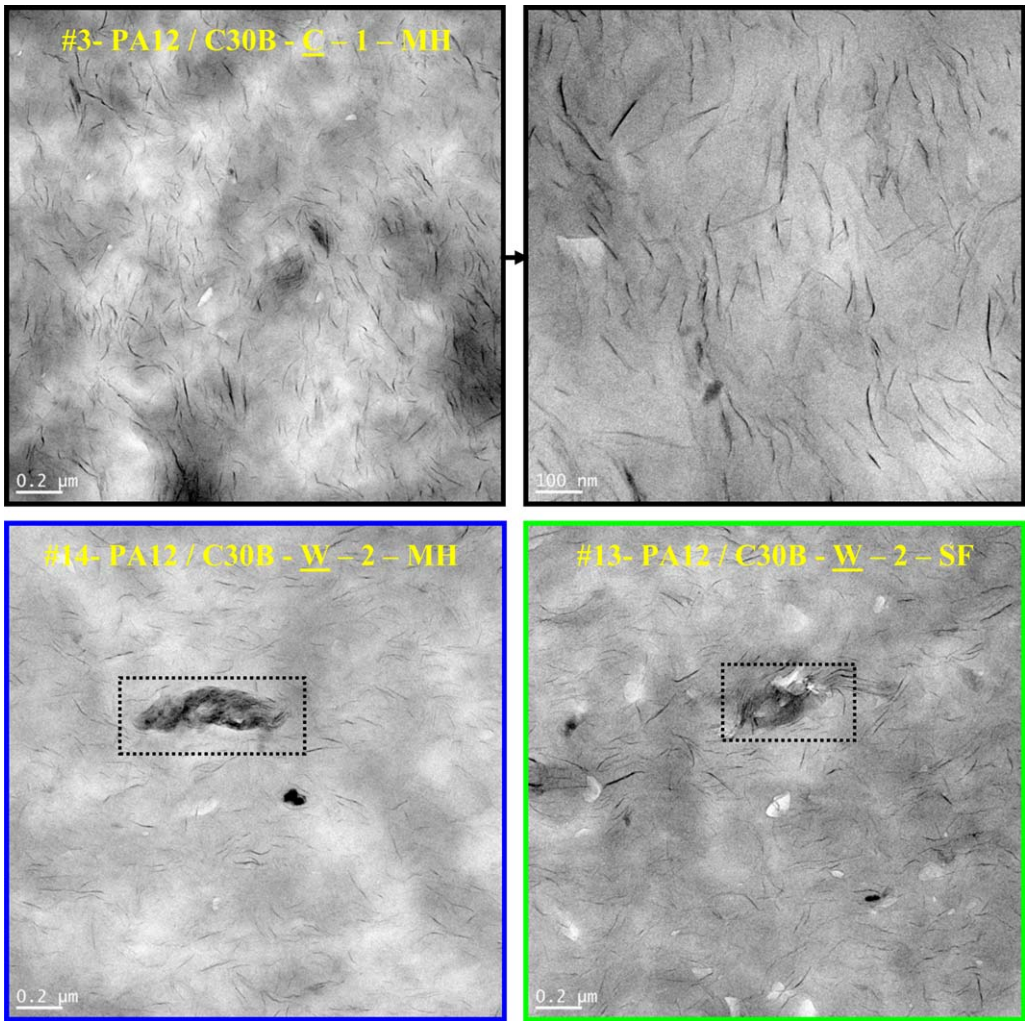

Figure 10. TEM photographs of PA12/Cloisite 30B composites prepared using various compounding strategies. A few larger tactoids can be observed in composites prepared using Method W. [Color figure can be viewed in the online issue, which is available at wileyonlinelibrary.com.]

composites exhibit an attenuation of the diffraction peak typical of partial exfoliation. Background subtraction enables to discern two diffraction peaks corresponding to two distinct populations of clay nanoparticles. The first peak is localized at low beam incidence angles (1.5°–1.2°, equivalent to 5.8–7.4 nm) and probably corresponds to exfoliated platelets. The second peak is localized around 5.8° and corresponds to clay tactoids with an interlayer spacing of 1.50 nm to 1.52 nm. Such a value is smaller than that of Cloisite 30B (d_{001} = 1.85 nm), indicating that a fraction of the organic intercalating agent might have been expelled from the galleries during compounding.[22–24] Using the equation proposed by Ishida et al.,[25] it was possible to estimate the degree of exfoliation (X_E) of PA12/Cloisite 30B composites:

$$X_E = 1 - \frac{A}{A_0} \quad (2)$$

where A and A_0 are respectively the areas of the clay diffraction peak in the nanocomposite and in the pure clay. Equation (1) is valid when the exfoliation process involves a broadening and a decrease in the intensity of the clay diffraction peak, which occur upon breakage of intercalated stacks and/or peeling of individual platelets or short stacks. The results, reported in Table IV show that X_E is very similar for all processing conditions, ranging from 77% (Method W, main hopper feeding) to 82% (Method C and Method W, side feeding). SEM photographs (Figure 9) confirm the absence of large microaggregates in all PA12/Cloisite 30B composites. Finally, TEM photographs (Figure 10) confirm the high extent of exfoliation. However, while the dispersion state at the nanoscale is very similar for all formulations, composites processed with Method C seem to exhibit less tactoids than their equivalents processed with Method W.

Oscillatory Rheometry

Oscillatory rheometry was used for two main purposes: (i) to evaluate the influence of water on the molecular weight of PA12 during extrusion compounding; and (ii) to indirectly probe the dispersion state of the clay in the composites. Complex viscosity and storage modulus were measured as a function of the frequency for unprocessed PA12, PA12 extruded under various conditions (samples #1, 5, and 6) and selected PA12/clay nanocomposites based on Cloisite Na^+ (sample #18) and Cloisite

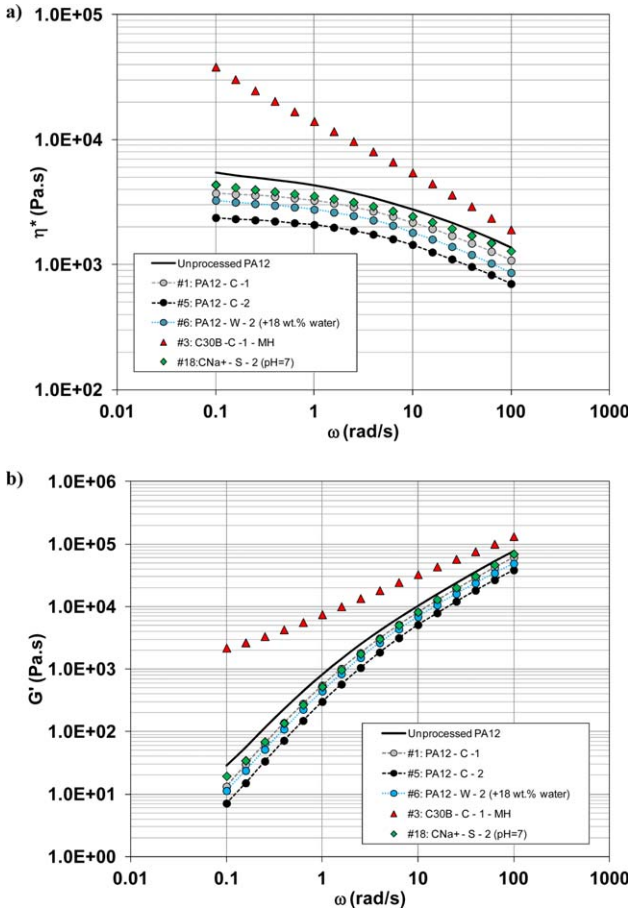

Figure 11. Rheological properties at 230°C of unprocessed PA12, PA12 extruded according to various conditions and selected PA12/clay nanocomposites: (a) complex viscosity (η^*); (b) storage modulus (G'). [Color figure can be viewed in the online issue, which is available at wileyonlinelibrary.com.]

30B (sample #3) (the latter formulations were chosen based on the results of clay dispersion analysis). Rheological curves are given in Figure 11.

The molecular weight of unprocessed PA12 and extruded PA12 samples was estimated through their zero-shear viscosity using the following method. Assuming the Cox-Merz rule valid, TA Orchestrator software was used to fit the viscosity data according to Carreau model:

$$\eta = \eta_0[1+(\lambda\dot{\gamma})^a]^{\frac{n-1}{a}} \quad (3)$$

where η_0 is the zero-shear viscosity, λ is a time constant, a is an exponent and n is the pseudo-plasticity index. Above the entanglement molecular weight, the zero-shear viscosity of linear entangled polymers is related to the average molecular weight (M_w) as follows[26]:

$$\eta_0 = KM_w^{3.4} \quad (4)$$

The parameter K of PA12 was calculated using the average molecular weight and the zero-shear viscosity of unprocessed PA12. Its value was 3.568×10^{-13} (Pa.s)/(g/mol)$^{3.4}$. This value was used to estimate the average molecular weight of samples #1, 5, and 6 using their zero-shear viscosity. It should be noted that this method is indirect and only provides an estimation of M_w. The results are given in Table V. Conventional extrusion leads to a significant molecular weight reduction, reaching from −13% for screw configuration 1 to −24 % for screw configuration 2. Indeed, screw configuration 2 has a more aggressive design, generating localized hot spots in zones 6, 8, and 9. Those hot spots are probably responsible for additional thermal degradation. Combination of screw configuration 2 and

Table V. Parameters of the Carreau Model and Estimated Molecular Weight for Unprocessed PA12 and PA12 Extruded According to Various Conditions

#	Matrix	Method	Screw configuration	η_0 (Pa.s)	λ	a	n	Fit error	M_w (g/mol)
-	Unprocessed PA12	-	-	6283	0.105	0.419	0.509	0.9995	60,000
1	PA12	C	1	3858	0.239	0.705	0.619	0.9999	51,981
5	PA12	C	2	2436	0.168	0.689	0.588	0.9996	45,409
6	PA12	W (18 wt % water)	2	3388	0.183	0.632	0.564	0.9992	50,035

Applied Polymer SCIENCE

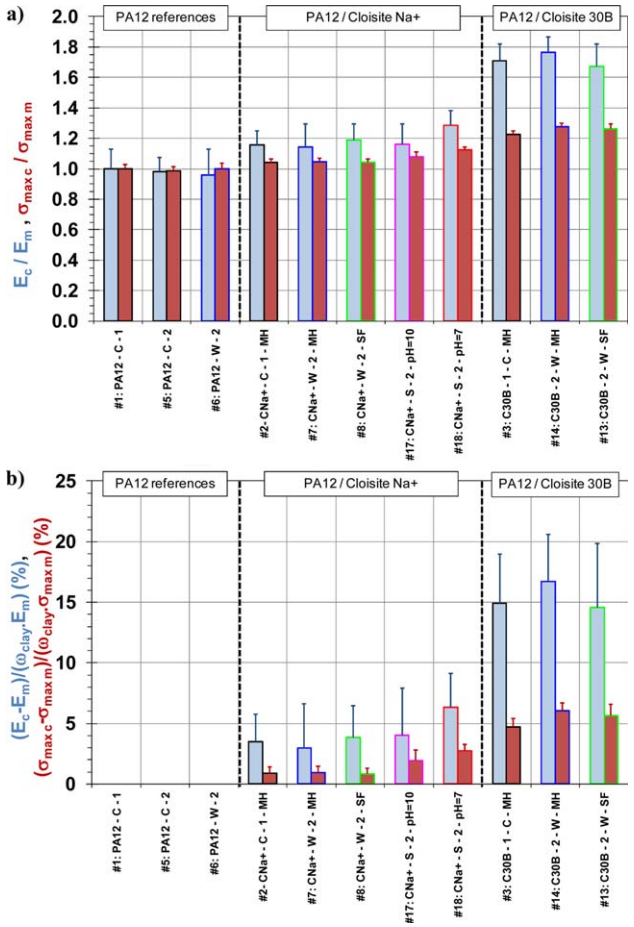

Figure 12. Relative tensile properties of extruded PA12 and PA12/clay nanocomposites (a) and improvement in tensile properties regarding clay mass fraction (b) [reference is PA12 conventionally extruded using screw configuration 1 (sample #1), for which E = 1616 MPa and σ_{max} = 46 MPa]. [Color figure can be viewed in the online issue, which is available at wileyonlinelibrary.com.]

addition of water (up to 18 wt %) does not generate any further molecular weight reduction. This might either indicate that hydrolysis is not significant, or that it is compensated by a reduction of thermal degradation, as the hot points are eliminated by the injection of cold water. Overall, those results are consistent with previous studies involving PA6[5,7] or copolyetheramide,[14] which concluded that hydrolysis during water-assisted extrusion processes remained limited, essentially due to short contact times between polymer and water.

The measurement of the viscoelastic properties of PA12/clay selected composites also allowed for an indirect confirmation of their dispersion state. As seen in Figure 11, PA12/Cloisite 30B

Table VI. Average Aspect Ratio of Clay Particles in Composites as Determined from Tensile Modulus Data and Halpin-Tsai Model

#	Sample	Inorganic content (wt %)	E_c/E_m (experimental)	Aspect ratio (theoretical)
1	PA12	-	1	-
2	PA12/Cloisite Na^+—C—1—MH	4.54	1.16	4.8
7	PA12/Cloisite Na^+—W—2—MH	4.78	1.14	3.8
8	PA12/Cloisite Na^+—W—2—SF	4.90	1.19	5.3
17	PA12/Cloisite Na^+—S—2 (pH = 10)	4.04	1.16	5.5
18	PA12/Cloisite Na^+—S—2 (pH = 7)	4.48	1.28	9.6
3	PA12/Cloisite 30B—C—1—MH	4.75	1.71	32.8
14	PA12/Cloisite 30B—W—2—MH	4.57	1.76	39.5
13	PA12/Cloisite 30B—W—2—SF	4.63	1.67	31.1

nanocomposites exhibit a drastic increase in viscosity and storage modulus at low frequencies, consistent with the formation of a percolated structure. On the contrary, PA12/Cloisite Na^+ composites do not show any significant difference in rheological properties compared with extruded PA12, which is typical of conventional microcomposite structures. Those results are consistent with WAXD conclusions and microscopical observations.

Tensile Properties

The relative tensile modulus and maximum tensile stress of PA12/clay nanocomposites compared with extruded PA12 are given in Figure 12(a). The improvements compared with extruded PA12 are also reported in Figure 12(b) as a function of the actual clay content. Despite the molecular weight reduction revealed by oscillatory rheometry, the tensile properties of extruded PA12 were not significantly impacted by the use of screw configuration 2 nor by the addition of water (up to 18 wt %). PA12/Cloisite Na^+ composites prepared using Method C showed a 14% increase in tensile modulus and a 4% increase in maximum tensile stress compared with pure PA12. Such a limited performance is not surprising taking into account the coarse dispersion of the clay particles, as revealed by microscopy. No further significant improvement was observed for composites prepared using Method W and Method S (pH = 10). However, the formulation prepared using Method S and the neutralized clay slurry (pH = 7) showed a significant improvement with a 28% increase in tensile modulus and a 12% increase in maximum tensile stress compared with pure PA12. This result is in accordance with the finer clay dispersion and the presence of individual platelets, as revealed by image analysis and WAXD. Finally, PA12/Cloisite 30B nanocomposites prepared by various methods exhibit less variation in their tensile properties. They show a 67% to 76% increase in tensile modulus and a 22% to 28% increase in maximum tensile stress compared with PA12. Although not shown here, the elongation at break of PA12 ($\varepsilon_b \approx 400$ %) was reduced by the addition of clay particles. However, it was maintained between 200% and 300% for PA12/Cloisite Na^+ composites, and between 100% and 300% for PA12/Cloisite 30B nanocomposites.

Based on the experimental data, the model of Halpin-Tsai[27] was used as a first approximation to estimate the average aspect ratio of clay particles in PA12/Cloisite Na^+ composites. Density of montmorillonite particles was set to 2860 kg/m^3. Elastic modulus of montmorillonite was taken equal to 170 GPa.[28] Actual montmorillonite content, as determined by TGA, was used to perform the calculation. The results are shown in Table VI. In the case of PA12/Cloisite Na^+ composites, the variations observed in tensile modulus correspond to an increase of the average aspect ratio of the clay particles from 4.8 (Method C) up to 9.6 (Method S; pH = 7), i.e., a 100 % increase in average aspect ratio. Those values are higher than those experimentally determined by image analysis of SEM photographs (Table III). This is consistent with the fact that the analysis was performed only on clay microparticles and does not take into account smaller particles such as tactoids or individual clay layers. It should be noted that, as expected, PA12/Cloisite Na^+ composites prepared with Method W exhibit a slightly higher aspect ratio of clay particles when side feeding rather than main hopper feeding is used. Finally, in the case of PA12/Cloisite 30B composites, tensile modulus values correspond to an average aspect ratio of the clay particles comprised between 31 and 40. Those values are consistent with the size of the tactoids observed on Figure 10.

CONCLUSIONS

PA12 composites based on untreated montmorillonite were prepared using conventional extrusion (Method C) and water-assisted extrusion processes involving injection of water (Method W) or injection of aqueous clay slurry (Method S) in the main polymer stream. It was shown that water-assisted extrusion processes allow for a significant enhancement in clay dispersion compared with conventional extrusion, with Method S leading to the finest micro-dispersion. Prior neutralization of the slurry using a strong acid allows for a modification of the interactions between individual clay platelets in the aqueous medium. This results in a better pre-exfoliation of the clay platelets in the slurry and hence, in a better dispersion of the clay micro and nanoparticles in the final composite. Overall, at the macroscopic level, the use of Method S combined with neutralization of the clay slurry leads to a 46% decrease in clay microparticles mean area and a 100% increase in aspect ratio compared with conventional compounding. This generates an additional ca. 10% increase in tensile properties. Such a moderate increase in mechanical properties is consistent with the fact that clay particles remain essentially dispersed at the microscale, which does not allow to achieve high aspect ratios. Control PA12/Cloisite 30B samples were also prepared using Method C and Method W. An extent of exfoliation of ca. 80% was measured in those composites almost independently of the processing method used and of the clay feeding location. In this specific case, the improvement in dispersion and in macroscopic properties brought by Method W was found to be insufficient to justify its use over conventional compounding.

This study confirms the potential of water-assisted extrusion processes to significantly enhance the dispersion state in PA12/untreated montmorillonite composites. However, despite a drastic reduction in clay microparticles size, improvements in mechanical properties remained limited, due to the fact that clay remained mainly dispersed at the microscale. Therefore, the use of water-assisted processes should be restricted to the preparation of composites based on untreated inorganic particles, devoted to applications for which the presence of an organic intercalating agent is highly undesirable.

ACKNOWLEDGMENTS

The authors are grateful to NRC technical officers Florence Perrin-Sarazin, Pierre Sammut, and Manon Plourde for their assistance with microscopy, rheological characterization, and mechanical testing, respectively, and to NRC research officer Nathalie Chapleau for the revision of the manuscript.

REFERENCES

1. Pérez, J.; Bax, L.; Escolano, C. Willems & van den Wildenberg (W & W España), Roadmap Report on Nanoparticles.

2005. Available at: http://nanoparticles.org/pdf/PerezBaxEscolano.pdf. Last accessed on: July 5, 2012.

2. Shah, R. K.; Paul, D. R. *Polymer* **2006**, *47*, 4075.
3. Stoeffler, K.; Lafleur, P. G.; Denault, J. *Polym. Degrad. Stab.* **2008**, *93*, 1332.
4. Korbee, R. A.; Van Geenen, A. A. Pat. WO 9,929,767 (**1999**).
5. Yu, Z.-Z.; Hu, G.-H.; Varlet, J.; Dasari, A.; Mai, Y.-W. *J. Polym. Sci. Part B: Polym. Phys.* **2005**, *43*, 1100.
6. Dasari, A.; Yu, Z.-Z.; Mai, Y.-W.; Hu, G.-H.; Varlet, J. *Compos. Sci. Technol.* **2005**, *65*, 2314.
7. Fedullo, N.; Sclavons, M.; Bailly, C.; Lefebvre, J.-M.; Devaux, J. *Macromol. Symp.* **2006**, *233*, 235.
8. Molajavadi, V.; Garmabi, H. *J. Appl. Polym. Sci.* **2011**, *119*, 736.
9. Kato, M.; Matsushita, M.; Fukumori, K. *Polym. Eng. Sci.* **2004**, *44*, 1205.
10. Aloui, M.; Soulestin, J.; Lacrampe, M.-F.; Krawczak, P.; Rousseaux, D.; Marchand-Brynaert, J.; Devaux, J.; Quiévy, N.; Sclavons, M. *Polym. Eng. Sci.* **2009**, *49*, 2276.
11. Rousseaux, D. D. J.; Sallem-Idrissi, N.; Baudouin, A.-C.; Devaux, J.; Godard, P.; Marchand-Brynaert, J.; Sclavons, M. *Polymer* **2011**, *52*, 443.
12. Lecouvet, B.; Sclavons, M.; Bourbigot, S.; Devaux, J.; Bailly, C. *Polymer* **2011**, *52*, 4284.
13. Mainil, M.; Urbanczyk, L.; Calberg, C.; Germain, A.; Jerome, C.; Bourbigot, S.; Devaux, J.; Sclavons, M. *Polym. Eng. Sci.* **2010**, *50*, 10.
14. Touchaleaume, F.; Soulestin, J.; Sclavons, M.; Devaux, J.; Cordenier, F.; van Velthem, P.; Flat, J. J.; Lacrampe, M. F.; Krawczak, P. *Express Polym. Lett.* **2011**, *5*, 1085.
15. Hasegawa, N.; Okamoto, H.; Kato, M.; Usuki, A.; Sato, N. *Polymer* **2003**, *44*, 2933.
16. Newman, A. C. D. Chemistry of Clays and Clay Minerals; Wiley-Interscience: New York, **1988**.
17. Chang, S. H.; Ryan, M. H.; Gupta, R. K. *Rheol. Acta* **1993**, *32*, 263.
18. Tombácz, E.; Szekeres, M. *Appl. Clay Sci.* **2004**, *27*, 75.
19. Dennis, H. R.; Hunter, D. L.; Chang, D.; Kim, S.; White, J. L.; Cho, J. W.; Paul, D. R. *Polymer* **2001**, *42*, 9513.
20. Grim, R. E. Clay Mineralogy, 2nd ed.; McGraw-Hill: New York, **1968**.
21. Utracki, L. A. Clay-Containing Polymeric Nanocomposites; Rapra Publishing, Shawbury, Shrewsbury, Shropshire, United Kingdom, **2004**; Vol. *2*, 785 p.
22. Yano, K.; Usuki, A.; Okada, A. *J. Polym. Sci. Part A: Polym. Chem.* **1997**, *35*, 2289.
23. Lan, T.; Kaviratna, P. D.; Pinnavaia, T. J. *Chem. Mater.* **1994**, *6*, 573
24. Alexandre, M.; Dubois, P. *Mater. Sci. Eng. R: Rep.* **2000**, *28*, 1.
25. Ishida, H.; Campbell, S.; Blackwell, J. *Chem. Mater.* **2000**, *12*, 1260.
26. Fox, T. G., Jr.; Flory, P. J. *J. Phys. Colloid Chem.* **1951**, *55*, 221.
27. Halpin, J. C.; Kardos, J. L. *Polym. Eng. Sci.* **1976**, *16*, 344.
28. Chen, B.; Evans, J. R. G. *Scripta Mater.* **2006**, *54*, 1581.